Resonant chalcogenide-metal-fluoropolymer nanograting for tunable pyroelectric sensing

Le Wei[1], Jingjing Qian[1], Liang Dong[1,*], and Meng Lu[1,2,*]
[1]*Department of Electrical and Computer Engineering, Iowa State University, Ames, IA 50011*
[2]*Department of Mechanical Engineering, Iowa State University, Ames, IA 50011*
**Email: ldong@iastate.edu and menglu@iastate.edu*

Abstract: A resonant pyroelectric detector was demonstrated to support narrowband and tunable photopyroelectric effect in the near-infrared region. The narrowband pyroelectric device was built on a chalcogenide-metal-fluoropolymer (As_2S_3-Ag-PVDF) nanograting membrane, which was fabricated inexpensively using a solvent-assisted imprint lithography process. Under the resonant condition, the device exhibited a responsivity of 1.36 V/W. The device's absorption and pyroelectric characteristics can be tuned using a bias voltage applied to the membrane.

OCIS codes: (230.0230) Optical device; (140.4780) Optical resonator; (050.5298) Photonic crystal; (010.1030) Absorption.

1. Introduction

A photopyroelectric detector can absorb electromagnetic radiation and generate transient pyroelectric voltage as a response to its temperature change [1]. Different types of photopyroelectric detectors have been developed to measure the change of optical signal in a broad spectral range from visible to terahertz [2, 3]. In contrast to the broadband devices, narrowband photopyroelectric devices, which show a higher sensitivity at a specific wavelength range, can be implemented to provide spectral information [4-6]. Here, we demonstrate the on-chip integration of a photonic crystal structure and a pyroelectric membrane. For applications in near- and mid-infrared, the photonic crystal was fabricated using chalcogenide glasses (As_2S_3) to archive a narrow bandwidth and a high-quality factor [7].

2. Results and discussion

Fig. 1(a) shows the structure of the R-PED built upon a 15-μm-thick polyvinylidene fluoride-trifluoroethylene (PVDF-TrFE) membrane with the one-dimensional grating pattern. The grating was patterned into the PVDF-TrFE thin film using a solvent-assisted imprint lithography process. On the top of the gating, the 100-nm silver (Ag) and 300-nm As_2S_3 films were deposited. The bottom side of the PVDF-TrEF membrane was coated using a 100-nm-thick Ag layer. These two Ag layers of silver were used as electrical contacts. Under an optical excitation, the Ag-As_2S_3 grating functions as a resonant absorber to absorb the light, generate heat and raise the membrane temperature. The change of the membrane temperature can generate a pyroelectric voltage (PEV) output. In a heating phase, the PEV signal increases until the temperature reach equilibrium, as shown in Fig. 1(b). During a cooling phase, the device output an opposite PEV signal. Owing to the guided-mode resonance effect, the Ag-As_2S_3 grating can selectively absorb near-infrared radiation, also known as on-resonance absorption, to generate a stronger PEV signal than the off-resonance case (Fig. 1(b)).

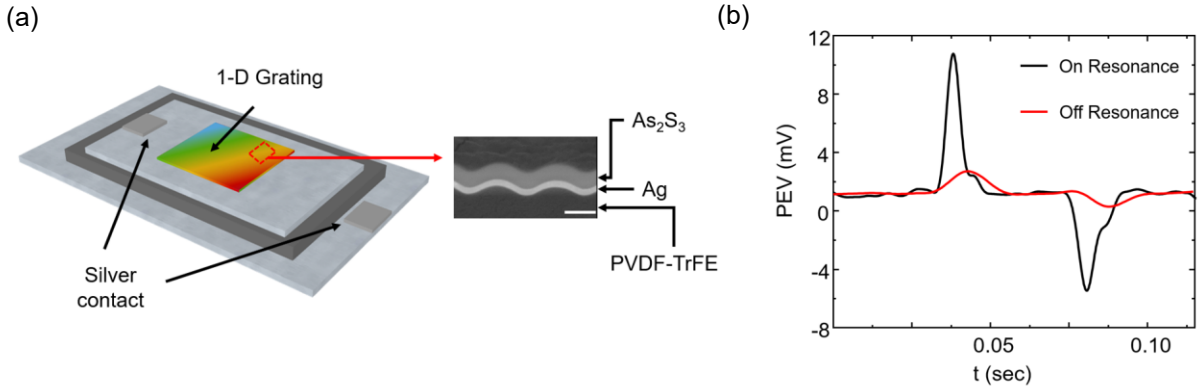

Fig. 1 Design and operation of the tunable R-PED. (a) Schematic diagram of the R-PED and a cross-sectional SEM image of the fabricated R-PED structure. Scale bar: 500 nm. (b) Pyroelectric sensor output using for on-resonance and off-resonance operations, respectively.

To characterize the fabricated R-PED, we mounted the sample on a rotation stage to control the angle of incidence (θ_i). A tunable near-infrared laser was used as the excitation source, and the PEV signals were measured using an oscilloscope connected across the PVDF-TrFE membrane. Fig 2(a) plots the PEV output as a function of time when the excitation laser (λ = 1560 nm, P = 7.26 mW) was modulated using a 50-ms-period square wave. The read and blue regions in Fig. 2(a) correspond to the on and off states of the laser. The spectral responsivities of the R-PED were

measured at θ_i = 0°, 5°, and 10°, as shown in Fig. 2(b). At each angle, the laser wavelength was scanned from 1520 nm to 1620 nm with an increment of 5 nm. It can be seen from Fig. 2(b) that the PEV output strongly depends on the coupling to resonant mode. Fig. 2(c) compares the PEV signal as a function of the laser power for on-resonance (θ_i = 0° and λ_i = 1560 nm) and off-resonance (θ_i = 10° and λ_i = 1560 nm) cases. The on-resonance input-output relationship showed a slope of 1.36 V/W, which is 45 times higher than the off-resonance slope of 0.03 V/W.

Fig. 2 Characterization of the R-PED's PEV response. (a) Measured PEV outputs as a function of time. (b) Measured R-PED responsivity versus wavelength. (c) Measured TEV outputs as a function of laser power when the incident angle is 0° and 10°.

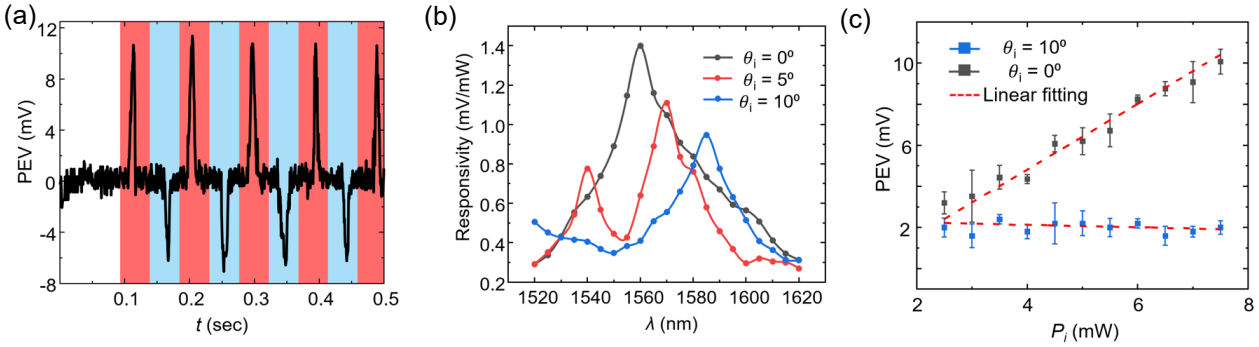

As a piezoelectric material, the PVDF-TrFE membrane can generate mechanical stress when a bias voltage is applied across it. The strain mismatch between the PVDF-TrFE membrane and Ag/As_2S_3 thin films can bend the membrane, as illustrated in Fig. 3(a), where φ is the bending angle. Fig. 3(b) compares the measured absorption spectra with the bias voltage ranging from 0 to 20 V. It can be seen from Fig.3 (b) that the absorption of the device for a fixed wavelength, especially 1560 nm, will decrease. Then, we repeated the experiment when the device was connected to an external voltage. Without a bias, the absorption resonance resided at λ_r = 1560 nm. The bias voltage can deform the membrane and alter the grating period as well as θ_i. As a result, the resonance mode split and shifted in the way given by the device's dispersion relationship. To demonstrate the tunable pyroelectric effect, we applied the DC bias voltage to deform the membrane and measure its PEV outputs. Without the bias voltage, the device can absorb the laser light efficiently and generate a strong PEV output of 10.2 mV. When the bias increased from 0 V to 15 V, the device absorption was reduced, and the PEV output consequently decreased from 10.2 mV to 2.9 mV.

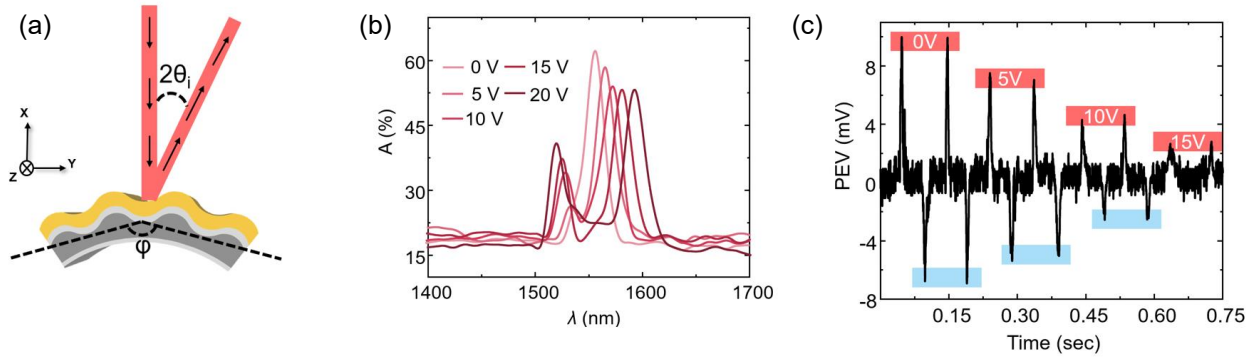

Fig. 3 Tuning of absorption resonance by biasing the PVDF-TrFE membrane. (a) Schematic diagram of the absorption spectra measurement when a DC bias is applied. (b) Measured absorption spectra with the bias voltage of 0 – 20 V. (c) PEV output measured during eight heating/cooling cycles with different bias voltages.

References:

1. Whatmore, R. W. "Pyroelectric devices and materials." *Reports on progress in physics* 49.12 (1986): 1335.
2. Zorin, Ivan, et al. "Mid-infrared Fourier-domain optical coherence tomography with a pyroelectric linear array." *Optics Express* 26.25 (2018): 33428-33439.
3. Yang, Jun, Shuangchen Ruan, and Min Zhang. "Real-time, continuous-wave terahertz imaging by a pyroelectric camera." *Chinese optics letters* 6.1 (2008): 29-31.
4. Suen, Jonathan Y., et al. "Multifunctional metamaterial pyroelectric infrared detectors." *Optica* 4.2 (2017): 276-279.
5. Liu, Longju, et al. "A phase-change thin film-tuned photonic crystal device." *Nanotechnology* 30.4 (2018): 045203.
6. Monshat, Hosein, Longju Liu, and Meng Lu. "A Narrowband Photo-Thermoelectric Detector Using Photonic Crystal." *Advanced Optical Materials* 7.3 (2019): 1801248.
7. Wei, Le, et al. "Chalcogenide Photonic Crystals Fabricated by Soft Imprint-Assisted Photodoping of Silver." *Small* 16.19 (2020): 2000472.